HHS Public Access

Author manuscript

Cancer Prev Res (Phila). Author manuscript; available in PMC 2017 May 01.

Published in final edited form as:

Cancer Prev Res (Phila). 2016 May ; 9(5): 367–378. doi:10.1158/1940-6207.CAPR-15-0107.

Mammary Adipose Tissue-derived Lysophospholipids Promote Estrogen Receptor-negative Mammary Epithelial Cell Proliferation

Paul A. Volden[1], **Maxwell N. Skor**[1,5], **Marianna B. Johnson**[1], **Puneet Singh**, **Feenalie N. Patel**, **Martha K. McClintock**[2,4], **Matthew J. Brady**[1,5,#], and **Suzanne D. Conzen**[1,3,4,5,#]

[1]Department of Medicine, The University of Chicago, Chicago, IL

[2]Department of Psychology, The University of Chicago, Chicago, IL

[3]Ben May Department of Cancer Research, The University of Chicago, Chicago, IL

[4]Institute for Mind and Biology, The University of Chicago, Chicago, IL

[5]Committee on Molecular Metabolism and Nutrition, The University of Chicago, Chicago, IL

Abstract

Lysophosphatidic acid (LPA), acting in an autocrine or paracrine fashion through G protein-coupled receptors, has been implicated in many physiological and pathological processes including cancer. LPA is converted to lysophosphatidylcholine (LPC) by the secreted phospholipase, autotaxin (ATX). Although various cell types can produce ATX, adipocyte-derived ATX is believed to be the major source of circulating ATX and also to be the major regulator of plasma LPA. In addition to ATX, adipocytes secrete numerous other factors (adipokines); although several adipokines have been implicated in breast cancer biology, the contribution of mammary adipose tissue-derived LPC/ATX/LPA (LPA-axis) signaling to breast cancer is poorly understood. Using mammary fat-conditioned medium, we investigated the contribution of LPA signaling to mammary epithelial cancer cell biology and identified LPA signaling as a significant contributor to the oncogenic effects of the mammary adipose tissue secretome. To interrogate the role of mammary fat in the LPA-axis during breast cancer progression, we exposed mammary adipose tissue to secreted factors from estrogen receptor-negative mammary epithelial cell lines and monitored changes in the mammary fat pad LPA-axis. Our data indicate that bidirectional interactions between mammary cancer cells and mammary adipocytes alter the local LPA-axis and increase ATX expression in the mammary fat pad during breast cancer progression. Thus, the LPC/ATX/LPA axis may be a useful target for prevention in patients at risk of ER-negative breast cancer.

[#]To whom correspondence should be addressed at: The Knapp Center for Biomedical Discovery, 8th Floor, 900 East 57th Street, Chicago, IL 60637, sdconzen@uchicago.edu or mbrady@medicine.bsd.uchicago.edu.

Disclosures: none

Keywords

adipocyte; lysophosphatidic acid; autotaxin; triple-negative breast cancer; microenvironment; mammary fat; phospholipid

Introduction

Cancer progression requires both cell-autonomous effects, specified by the genomes of cancer cells, and paracrine signals derived from the cells within the adjacent tumor stroma. Over the past decade, increasing effort has been made to identify stroma-derived signals that contribute to cancer progression and may be targets for cancer prevention. These efforts have sought to identify targets for intervention that may be less susceptible to the acquired epigenetic and genome alterations that are characteristic of genetically unstable cancer cells (1). Importantly, the paracrine interactions that influence cancer progression are dependent on the unique cellular and structural components of the microenvironment in which a particular cancer is located. In breast cancer, the mammary gland is increasingly appreciated as relatively unique, in large part due to the embedded nature of the mammary ductal tree and its cancer-prone epithelial cells within an adipocyte-laden microenvironment.

Prior to the mid-1990s fat cells were viewed simply as inert energy storage vessels, and more recently have become recognized as important endocrine cells. We also now know that adipocytes define a diverse and dynamic cell population with phenotypic properties specific to their anatomic location (2-4). For example, adipocytes possess aromatase activity and can increase localized and systemic levels of estrogen (5). Consistent with this finding, increased adiposity has been positively associated with estrogen receptor-positive (ER+) breast cancer risk in post-menopausal women (6). Furthermore, numerous studies have described breast cancer-promoting effects of adipokines, predominantly those deregulated in obesity (7). However, few investigations have directly addressed the influence of mammary adipocyte-derived signals on triple-negative breast cancer (TNBC: tumors lacking ER, progesterone receptor and HER2 expression). This is surprising considering the frequent proximity of adipocytes to mammary epithelium, the necessity for mammary adipocyte signals for normal mammary ductal development (8-10), and new data demonstrating phenotypic differences between distinct fat depots. Given the aggressiveness of TNBC and the lack of preventive treatments, increasing our understanding of the interaction between mammary adipocyte physiology and TNBC progression is important. Potentially, research in this area could identify novel biomarkers for TNBC progression and targets for intervention.

In the SV40 T-antigen (TAg) transgenic mouse model of human TNBC, the chronic stress response following long-term social isolation of female mice has been associated with a larger mammary gland tumor burden and increased tumor invasiveness compared to female mice developing in a socially enriched, group-housed environment (11). We previously reported that exposure to this form of chronic social stress is also associated with upregulation of genes mediating conversion of glucose to lipids in mammary adipocytes of female SV40 TAg mice, and a concomitant increase in *de novo* lipid synthesis (12). Furthermore, serum-free medium pre-incubated with mammary fat (conditioned medium)

caused significantly augmented proliferation of Tag mouse mammary epithelial cells (MECs) (12). These data suggested that alterations in mammary adipocyte metabolism and associated changes in the mammary fat secretome could alter the local microenvironment and contribute to TNBC progression.

Here we report that in SV40 TAg female mice, phospholipid profiling of mammary adipose tissue-derived lipids revealed a dramatic increase in lysophosphatidylcholine (LPC) in the mammary fat of socially isolated vs. group-housed mice. LPC is a phospholipid precursor to the proliferative signaling molecule lysophosphatidic acid (LPA). LPA acts through specific G-protein-coupled receptors and has been implicated in diverse pathological processes, including breast cancer progression (13-16). LPA is primarily generated from an LPC precursor by the enzymatic action of the secreted phospholipase, autotaxin (ATX). Although breast cancer cells can produce ATX, adipocytes are believed to be the major source of circulating ATX and the major regulator of plasma LPA concentrations (17,18). These data suggest that mammary stromal adipocytes could be significantly contribute LPC/LPA/ATX-axis signaling.

To evaluate the hypothesis that lysophospholipids originating from local mammary adipocytes influence ER- breast cancer progression, we examined the contribution of LPC and LPA to the cell proliferative and survival effects of the mammary adipose tissue secretome. Our data identify both LPC and LPA as significant contributors to the oncogenic effects of the mammary adipose tissue secretome and suggest multiple important roles for adipocyte-derived lysophospholipids in TNBC progression. We also show that TAg MECs are associated with increased expression of ATX in the mammary fat pad. Taken together, these observations support further investigation into LPA-axis signaling and mammary adipocyte/epithelial crosstalk as a target for TNBC prevention efforts.

Materials and Methods

Animals and cell lines

All animal protocols conformed to the National Institutes of Health and the University of Chicago Animal Care Guidelines. Female FVB/N mice homozygous for the SV40 TAg transgene were provided by Dr. Jeff Green of the National Cancer Institute's Mouse Models of Cancer Consortium. Non-transgenic FVB/N mice were obtained from the Jackson Laboratory at 14 weeks of age. A set of isolated and grouped TAg mice cohorts provided mammary tissue used in lipid profiling experiments (n=4, grouped; n=6, isolated), and protocols for these mice were described previously (11). The SV40-TAg M28N2, M27H4, and M6 mammary cell lines were generously provided by Dr. Cheryl Jurcyk of Boise State University and have been described previously (19). The cell lines were authenticated by microscopic morphological analysis, were routinely tested with growth curve comparison to the original series of cell lines, and tested negative for mycoplasma by PCR-based analysis (ATCC 30-1012K™). To diminish the effects of continued passage on the cell lines, the cells were discarded after 20 passages.

Mammary fat-conditioned medium

Mammary fat pads were harvested from TAg mice at 14-17 weeks of age, and then finely minced in serum-free culture medium (Hyclone, SH30240.01). To enrich for adipose tissue, the samples were then centrifuged at 100 × *g* for 1 min and then the floating tissue was separated from pelleted tissue, weighed, and then incubated with medium (SH30240.01, Hyclone), containing 1% bovine serum albumin (BSA) and 1% penicillin/streptomycin (P/S), at 10mL medium per gram tissue and 37°C for 8 hours. Medium was then harvested and sterile-filtered through a 0.22 μm syringe filter, aliquoted, and then stored at −80 °C until use. All medium was thawed at 4°C or on ice prior to use in experiments. Frozen medium samples from 4 individual mice were shipped on dry ice to the Wayne State Lipidomics Core Facility for liquid chromatography-mass spectrometry (LC-MS, see Supplemental Methods).

Cell proliferation and cell death

Proliferation and cell death were monitored using the Incucyte™ live content imaging system. The Incucyte system periodically captures phase-contrast and fluorescence images from individual wells of tissue culture plates. Accompanying software allows the user to mask phase and fluorescent images in order to quantify the surface area covered by cells in a well (confluence as a surrogate for cell proliferation) and/or quantify fluorescence totals and object counts. YOYO-1 iodide fluorescently labels the nuclei of dead/dying cells and was used to quantify dead cells. To estimate cell numbers, a calibration curve was generated for each cell line. Cells were seeded by serial dilution into columns of a 96-well plate and the following day they were given either 5% FBS containing medium or mammary adipose tissue conditioned medium. After 8 hrs, confluence was obtained using the Incucyte system, and then cells were fixed with 10% trichloroacetic acid, followed by nuclear labeling with YOYO-1 and total cell counting using the Incucyte system. Cell numbers were plotted as a function of confluence and linear regression was used to model the data. The coefficient of determination for all cell line regression models was greater than 0.9. Cell numbers were calculated in subsequent experiments using respective linear models for each cell line. For all plots, the starting cell count at time=0 was subtracted from all subsequent values. Data were analyzed using a linear regression model with cell and percent dead counts from two independent experiments as the response variables. GraphPad Prism software was used to calculate a two-tailed P-value testing the null hypothesis that the slopes of the regression models for treatment conditions (e.g. dose vs. vehicle) were identical.

LPA signaling, LPC, and small molecule antagonists

LPA was purchased in ethanol from Cayman Chemical (LPA 18:1, 10010093). LPC was purchased from Avanti Polar Lipids (LPC 18:1, 845875P), dissolved in PBS with 1% BSA 2.5mM, and then stored in aliquots at −80 °C until use. Ki16425 (Cayman Chem., 10012659), H2L5186303 (Tocris Bio., 4878), and PF-8380 (Calbiochem, 189512) were purchased in DMSO solution and stored per manufacturer's recommendations. Solvents for LPA and small molecule antagonists contributed no more than 0.1% of the volume in all experiments. For LPA signaling assays, cells at roughly 75-90% confluence were serum-starved for 8 hrs prior to treatment. Cells were then dosed with LPA for ten minutes and then

washed with cold PBS, followed by protein harvesting and Western blot analysis, as described previously (20). LPA, LPC, and the antagonists used in proliferation/death experiments were added at the start of the experiments and medium were not changed for the experimental duration.

LPA receptor knockdown

SMARTpool: ON-TARGET plus siRNAs targeting mouse LPAr1-3 were purchased from Thermo Scientific. Reverse-transfection of siRNAs was performed using Opti-MEM and Lipofectamine RNAiMAX (Life Technologies) following methods previously described (21), with several modifications. Briefly, a transfection mix containing 250nM siRNA pool and 0.5% Lipofectamine was prepared and allowed to rest for 20 minutes. The mixture was then aliquoted in volumes of 20uL or 200uL to 96-well or 12-well plate, respectively. M28N2 and M27H4 cells were diluted in DMEM high glucose with 10% FBS to 2.5×10^4 or 1.9×10^4 cells/mL, respectively. The diluted cells were then added in 80uL volumes to 96-well plates or 400uL volumes to 12-well plates. Following 48 hrs of culture, RNA was harvested from the 12-well plate for later validation of targeted knockdown. Also at 48 hours, the medium in the 96-well plate was replaced with mammary adipose tissue conditioned medium and then the plate was placed in the Incucyte live content imaging system for the duration of the experiment.

Autotaxin IHC

Mammary fat pads were harvested from 15 week old female TAg mice and age-matched mice of the non-transgenic parental strain (n=4 per group). Fat pads were formalin-fixed for 24 hours immediately after necropsy and then embedded in paraffin. Sections (5 microns) were adhered to positively charged glass slides, de-waxed in xylene, and hydrated using graded ethanol washes. Heat-induced antigen retrieval was performed using Tris-EDTA Buffer (10mmol/L Tris base, 1 mmol/L EDTA solution, pH 9.0) incubation in a pressure cooker for 3 minutes. Immunostaining was performed using a 1:200 dilution of anti-ATX antibody (Millipore, ABT28) and a goat anti-rabbit secondary antibody (LI-COR 827-08365). Qualitative visual analyses were performed on scans of each section that were captured using the CRi Panoramic Whole Slide Scanner (PerkinElmer LifeSciences).

Quantitative RT-PCR

Messenger-RNA (1ug) was reverse-transcribed using the qScript cDNA synthesis kit (Quanta Biosciences). Quantitative real-time PCR was conducted with PerfeCTa SYBR Green FastMix (Quanta Biosciences). Statistical significance was determined using Student's t-test or, if multiple comparisons were performed, by one-way ANOVA on actin-normalized CT values. The mRNA expression of LPA receptor transcripts was determined using the standard curve based method of data processing (22). For all other transcripts analyzed, relative expression was determined using the Delta CT method (23). Primers used included *β-Actin*: 5'-AGAGGGAAATCGTGCGTGAC-3' (forward), 5'-CAATAGTGATGACCTGGCCGT-3' (reverse); *Scd1:* 5'-TTCTTGCGATACACTCT GGTGC-3' (forward), 5'-CGGGATTGAATGTTCT TGTCGT-3'(reverse); *Elovl6:* 5'-GAAAAGCAGT TCAACGAGAACG-3' (forward), 5'-AGATGCC GACCACCAAAGATA-3' (reverse); *ChREBPβ:* 5'-TCTGCAGATCGCGTGGAG-3'

(forward), 5’-CTTGTCCCGGCATAGCAAC-3’ (reverse); *ATX* (*Enpp2*): 5’-GACCCTAAAGCCATTATTGCTAA-3’ (forward), 5’-GGGAAGGTGCTGTTTCATGT-3’ (reverse); *LPAR1* (*Edg2*): 5’-GGACCTAGCAGGCTTACAGT-3’ (forward), 5’-TGCCAGGCACAAAAAGCAAT-3’ (reverse); *LPAR2* (*Edg4*): 5’-ACTACAACGAGACCATCGGC-3’ (forward), 5’-CGTGGGCCAGTATGGAACAT-3’ (reverse); *LPAR3* (*Edg7*): 5’-GGTGTCGAAAACGTTGACCG-3’ (forward), 5’-AGAGGCAATTCCATCCC AGC-3’ (reverse).

Lysophospholipid quantification

Phospholipid profiling was performed by the Kansas Lipidomics Research Center (KLRC) using an automated electrospray ionization (ESI)-tandem mass spectrometry approach as previously described (Deviah, et al. 2006) with modifications. Mammary adipose tissue was harvested from 15 week old female TAg mice. Upon harvest, adipose tissue was placed into a microcentrifuge tube containing DMEM high glucose medium with 1% penicillin/streptomycin. The tissue was then finely minced, spun at 100×g for 30 seconds, and the floating layer enriched in adipocytes was then transferred to a new pre-weighed tube. The remaining medium was then removed from beneath the tissue with a needle and syringe. Lipids were then extracted from the adipocytes using the Folch method. Briefly, 1mL of methanol was added to 100μL of adipose tissue. The adipocytes were then sonicated for 10 seconds at 6 watts. The entire volume was transferred to a Pyrex tube with Teflon cap. To the tube, 2 mL of chloroform were added and then the contents were allowed to shake and incubate for 10 minutes at ambient temperatures. Following addition of 850μL water and mixing, tubes sat for 10 minutes and then the lower phase was recovered. The upper phase was washed with 1.5 mL 86:14.1:1, CHCl3/methanol/water, v/v/v solvent mix and the lower phase was recovered and combined with the first recovery. To extract neutral lipids, the solvent was evaporated under nitrogen gas and lipids were re-suspended in 100uL of CHCl3. The solution was then added to a cyanopropyl solid phase extraction column (Fisher AT209550) that had been pre-rinsed with 10mL of hexane:ether:acetic acid, 80:20:1. Neutral lipids were eluted and collected off the column with a second 10mL volume of hexane:ether:acetic acid. Polar lipids were then collected off the column with a final wash of 10mL chloroform/methanol/water 4/1/0.1. The lipid fractions were then evaporated under nitrogen, weighed, and then shipped on dry ice to the Kansas Lipidomics Research Center for mass spectrometry profiling. Compound IDs were assigned based on the m/z of the intact ion and the mass of one fragment formed in the mass spectrometer. Signal peaks were compared to internal standards, which included 0.3 nmol LPC 13:0 and LPC 19:0. LPA was not detected because LC-MS lipid profiling was performed in positive ion mode ([M+H]+ ions) allowing for detection of LPC, but not LPA.

For targeted LPA and LPC analyses (conducted at Wayne State University), extracted samples were injected into a Targa C18 column (Higgins Analytical, Targa C18, 5μ, 10 × 2.1 mm) and eluted with a gradient between solvent A (Methanol : water : ammonium formate : formic acid; 5 : 95 : 2 mM : 0.2%) and solvent B (Methanol : ammonium formate : formic acid; 100 : 1 mM : 0.2%). The gradient program with respect to solvent B is: 0 min – 60%, 3 min – 100%, 6 min – 100% at a flow rate of 0.4 ml/min. The column was washed with 100% solvent B for 4 min at the end of each run and returned to initial conditions before next

injection. During analysis, samples were maintained at 15 °C and the column was maintained at 33 °C. Eluate from HPLC was directly introduced to the ion source of the mass spectrometer (ABSCIEX: QTRAP 5500). LPA were analyzed by Multiple Reaction Monitoring (MRM) for m/z 153 ion from each LPA species in the negative ion mode. LPC were analyzed similarly but following m/z 184 ion for each LPC species in the positive ion mode. *Mass spectrometer conditions are as follows:* Source temperature: 600 °C, *Curtain gas: 35* psi, GS1 and GS2: 45 psi, Ion Spray voltage: −4500 V (for LPA) or +5500 V (for LPC), Declustering Potential: −140 V or +100 V, Entrance Potential: −9 V or +10 V, Collision Energy: −30 eV or +37 eV, and Collision Cell Exit Potential: −7 V or +11V. Dwell time for each MRM transition was 25 ms with 5 ms interscan delay for a total scan time of 14 s in each duty cycle for a total of 24 LPA or LPC species. MRM data was analyzed by MultiQuant software (ABSCIEX) and each LPA or LPC was quantified against the internal standards, C17-LPA or C17-LPC, respectively.

Results

LPC is increased in mammary fat from socially isolated vs. group-housed SV40 TAg mice

We previously reported that the chronic stressor of early social isolation is associated with increased metabolic gene expression of several genes encoding important glucose flux and lipid metabolism proteins (hexokinase 2, ATP citrate lyase, and acetyl-CoA carboxylase alpha) within the mammary adipocytes of 15 week old female mice (12). Increased expression of these particular enzymes was predicted to increase glucose flux into lipid synthesis, which was confirmed (12). A subsequent analysis of our previously published microarray data (11) and quantitative real-time PCR revealed relatively increased expression of several additional lipid synthesis genes in socially-isolated animals' mammary glands, including stearoyl-CoA desaturase-1 (*Scd1*), the elongase ELOVL family member 6 (*Elovl6*), and carbohydrate-responsive element-binding protein β (*ChREBPβ*) (Supp. Fig. 1A).

Because the products of these genes have important roles regulating lipid synthesis and executing modifications to specific lipid species (24,25), we hypothesized that alterations in specific synthesized and secreted lipids from mammary adipocytes might be contributing to the larger tumor growth in social isolated versus grouped TAg mice. Therefore, we compared lipid profiles between the mammary fat pads of 15 week old socially isolated vs. grouped TAg mice in conjunction with the Lipidomics Core at Kansas State University. The most striking difference between the experimental groups was an approximate doubling of the LPC lipid species from socially isolated animals' mammary fat (Supp. Fig. 1B). LPA levels could not be directly measured using this lipidomics platform.

Mammary adipose tissue conditioned medium contains LPC and LPA and support the proliferation of TAg MECs

The data above suggested that the significantly higher LPC lipid species were present in the mammary fat from socially-isolated versus grouped female mice; combined with our previous data (12) demonstrating that isolated mice experience significantly greater mammary tumor growth compared to their group-housed counterparts, we wished to explore

possible mechanisms connecting high adipocyte LPC production to mammary tumorigenesis., This was of interest because LPC can be converted by the adipocyte-secreted enzyme ATX to the signaling species LPA, which in turn is known to activate epithelial proliferation signals through G-protein coupled receptors (18). We hypothesized that production of LPC in mammary adipocytes could lead to generation of oncogenic signaling affecting adjacent precancerous and cancerous MECs. To test this hypothesis, we tested a series of mammary cancer cell lines (M28N2, M27H4, and M6) derived from the TAg mouse model of human TNBC and representing progressive stages of breast cancer for their responsiveness to mammary fat-conditioned medium (19) (Fig.1A). M28N2, M27H4, and M6 cells were isolated from morphologically normal Tag mammary epithelium, *carcinoma in situ* (CIS), and an invasive tumor, respectively, and are referred to in this text by the stages from which they were obtained (i.e. “normal”, “CIS”, and “invasive”). These cells are unresponsive to estrogen and display properties, both *in vitro* and as xenografts, consistent with their representative stage of human TNBC progression (19).

Conditioned medium (CM) experiments have helped to identify adipokines, such as leptin and hepatocyte growth factor, as contributors to breast cancer progression (26,27). However, adipocytes secrete a plethora of growth factors, cytokines, and metabolites that likely contribute to the pro-tumorigenic signals observed in adipose tissue CM (2,28). Furthermore, adipose depots display metabolic and secretory properties that are specific to their anatomical location. Therefore, we next sought to develop a conditioned medium system that would best represent the mammary microenvironment and would allow us to determine whether or not LPA signaling is an important contributor to the overall pro-tumorigenic effects of mammary adipose tissue secreted factors.

To model the oncogenic effects of factors secreted locally by mammary adipocytes, we harvested mammary fat pads from TAg female mice, enriched them for mammary adipose tissue, and then made CM by incubating the minced fat samples in serum-free medium for 8 hours. When this medium was applied to TAg MEC cell lines, the CM was sufficient to support MEC proliferation and cell survival (Fig. 1B). With assistance from the lipidomics facility at Wayne State, we conducted targeted LPC and LPA analysis of the conditioned medium (Fig. 1C, Supp. Table 1). After 8 hrs, LPC concentrations in the CM were roughly 1uM and LPA concentrations averaged about 180nM.

LPA initiates both proliferative and cell survival signaling for TAg MECs

LPA has been reported to stimulate the proliferation and survival of numerous breast cancer cell lines (29), but the responsiveness of Tag-derived MECs to LPA has not been reported. Therefore, we first stimulated the cells with increasing doses of LPA and monitored phosphorylation of AKT, an established target of LPA signaling (30).

All cell lines displayed dose-responsive AKT phosphorylation starting in the low- to mid-nM range, which peaked around 2.5uM (Fig. 2A). Similar results were also observed for markers of ERK pathway activation upon LPA stimulation (data not shown). To determine whether LPA signaling affects cell proliferation and/or death in TAg MECs, we cultured the three cell lines in serum-free media and monitored their proliferation and cell death following LPA treatment. In the absence of serum for a 48hr period, all cell lines were

unable to sustain proliferation (Fig. 2B) but also underwent significant cell death (Fig. 2C). However, the addition of LPA both stimulated TAg MEC proliferation and protected them from cell death in a dose-dependent manner (Fig. 2B, C). These data suggest that LPA, at concentrations within the range measured in mammary CM, activates both proliferative and cell survival signaling in TAg MECs.

LPA signaling through LPA receptors (1 and 3) contributes to the pro-proliferative and anti-apoptotic effects of the mammary adipose tissue CM

LPA has been shown to interact with at least six known G protein-coupled LPA receptors (LPAR1-6). In Tag MECs, we determined the mRNA expression of the genes encoding LPA receptors 1, 2, and 3 (*edg1*, *edg4*, and *edg7*; respectively). These three LPAR isoforms have been implicated in breast cancer progression (14, 15, 31, 32). Transcripts for genes encoding all three receptors were detected (Fig. 3A); however, LPAR2 (*edg4*) mRNA was the most abundant within each cell line. We were unable to determine protein level expression of the LPARs due to ineffective antibodies, but we did obtain significant effects through blockade of LPAR signaling (below). Taken together these observations are concordant with the hypotheses that mammary adipose tissue contributes to LPA signaling in TNBC.

If LPA is a significant contributor to the pro-tumorigenic effects of the mammary adipose tissue secretome, antagonizing LPA signaling in TAg MECs cultured with mammary adipose CM would be expected to attenuate the secretome's proliferative and cell survival effects. To test this hypothesis, we used two small molecules to antagonize LPA signaling: H2L5186303, a specific inhibitor of LPAR2 (33); and Ki16425, which inhibits both LPAR1 and LPAR3 (34). In pilot experiments, both inhibitors displayed evidence of non-specific cytotoxicity at the 10uM concentration (data not shown). Therefore, we tested log dilutions, from 1uM down to 10nM, for their ability to antagonize the CM effects on MECs.

Antagonism of LPAR2 during culture with mammary adipose CM did not affect the proliferation of any of the TAg MECs, suggesting LPAR2, despite its relatively high expression, is dispensable for LPA's pro-proliferative effects (Fig. 3B), (Fig. 3A). However, the normal and CIS cell lines in CM were acutely sensitive to increasing doses of the LPAR1/3 antagonist (Fig. 3C). Notably, the anti-proliferative effects of the LPAR1/3 antagonist were not observed in cells cultured with 10% serum (Fig. 3D), suggesting the effects of the small molecule are specific and not the result of generalized toxicity. Interestingly, although the invasive cancer cell line was responsive to exogenous addition of LPA (Fig. 2B), the CM-induced proliferation of the invasive cancer cells was unaffected by the inhibitor, suggesting alternative factor(s) in the CM can promote proliferation through LPA-independent pathway(s) in these cells.

To confirm the chemical inhibitor results, we attempted siRNA-mediated knockdown of LPAR1 or LPAR3 in all three cell lines. In the normal and CIS cell lines that responded to LPAR1/3 antagonism, we were able to induce siRNA-mediated depletion of LPAR1 or LPAR3 expression (confirmed by quantitative real-time PCR) and these LPAR-depleted cells' behavior replicated the effects of the chemical inhibitor on intact cells (Fig. 4A). However, despite multiple attempts, we were unable to knockdown either LPAR1 or LPAR3 in the invasive TAg cells (data not shown). In the normal cell line, knockdown of either

LPAR1 or LPAR3 significantly attenuated the proliferative effects of the CM (Fig. 4B), suggesting that both receptors contribute to LPA-mediated pro-proliferative effects. Conversely, knockdown of LPAR1 in CIS cells had no effect on proliferation in CM, while LPAR3 knockdown dramatically antagonized the pro-proliferative effects of CM (Fig. 4B). Notably, although the overall percentage of cell death was low with the conditioned medium, knockdown of LPAR3 did result in a statistically significant increase in cell death in both cell lines (Fig. 4C). An increase in cell death was not observed with LPAR1 knockdown, suggesting that LPAR3 plays a unique role in cell survival. Taken together, these data support the small molecule inhibitor results, and suggest that LPA signaling dynamics may change during cancer progression.

LPC supports TAg cancer cell proliferation independently of LPAR signaling

Although adipocytes are believed to be the major source of circulating ATX (17), many cancer cells also express ATX (15, 35, 36). Because the LPA precursor, LPC, is also released by mammary adipocytes, we hypothesized that MEC autonomous conversion of mammary adipocyte-derived LPC to LPA could contribute to the cancer-promoting effects of the adipocyte secretome. To evaluate this hypothesis, we began by measuring the expression of ATX mRNA and protein in the progressively tumorigenic TAg MECs. All three cell lines expressed ATX and both ATX mRNA and protein levels were inversely associated with the stage from which each cell line was obtained (Fig. 5A, B).

To determine whether addition of LPC to serum-free medium could promote the proliferation and survival of TAg MECs, we stimulated the cells with increasing doses of LPC (0-40 uM) and monitored proliferation and cell death. LPC supported proliferation and survival in the normal and (at higher doses) the invasive TAg MECs; however, the effects of LPC were far less pronounced in the CIS cells (Fig. 5C, D). Interestingly, although the CIS cell line expressed intermediate levels of ATX and the invasive cell line the least amount of ATX, LPC was clearly more effective at stimulating proliferation and survival in the invasive cell line. These data suggest that the invasive cell line responds to LPC independently of LPAR-mediated signaling.

To test this hypothesis, we stimulated the LPC-sensitive cell lines (normal and invasive carcinoma) with LPC in the presence or absence of PF-8380 (40uM), a small molecule ATX antagonist (37). Inhibition of ATX activity in the normal cells eliminated the proliferative response to LPC (Fig. 5E). In contrast, ATX inhibition in the invasive cells did not alter the ability for LPC to promote cell proliferation (Fig. 5F). These data suggest that mammary adipocyte-derived LPC may support the growth of MECs with high ATX expression via LPA conversion (normal cells). LPC may also support invasive mammary cancer cells independently of ATX-mediated LPA generation and receptor signaling, although further work is required to prove this supposition.

TAg epithelial cell-secreted factors increase ATX expression in mammary adipose tissue

Recent studies have suggested that mammary tumorigenesis alters ATX expression within the mammary stroma (38). To determine whether increased stromal ATX expression is associated with progression to cancerous mammary epithelium, we performed anti-ATX

immunohistochemistry (IHC) on mammary fat pads harvested from 15 week old TAg FVB/N mice and compared them to age-matched non-transgenic FVB/N mice. Within the mammary stromal compartment, we observed striking differences in ATX staining between the transgenic and FVB/N mammary glands (Fig. 6A). Qualitatively, TAg mouse mammary fat pads stained much more intensely for ATX and the adipocytes tended to be smaller. These data agree with previous studies suggesting that mammary tumorigenesis increases ATX expression in the mammary stroma (32,38).

To test the hypothesis that paracrine signaling from TAg MECs increases ATX expression in the mammary fat pad, we began by generating CM from each of the TAg MECs. The MEC CM were then applied separately to mammary adipose tissue for 24 hr, after which mammary fat RNA and protein was harvested to measure ATX expression (Fig. 6B). Treatment of mammary adipose tissue with TAg MEC CM resulted in upregulation of the gene encoding ATX and a concomitant increase in ATX protein expression (Fig. 6C, D). These data support a model in which paracrine signals from TAg MECs augment ATX expression in the mammary fat pad, which in turn increase LPA production to promote TNBC proliferation.

Discussion

Prior studies have demonstrated that mammary fat-derived as well as other subcutaneous adipocytes secrete factors capable of influencing breast cancer biology (39). However, previous work has largely focused on estrogen and other adipokines affecting ER+ breast cancer (5,40-43). For example, studies that have examined the association between obesity and breast cancer risk have focused on ER+ mammary tumors, circulating adipokines that increase in obesity such as leptin, or aromatase activity and estrogen exposure in postmenopausal women (5,40-43). Additional studies have observed that obesity results in increased ATX expression within adipose tissue (44), decreased circulating LPC (45), and increased circulating LPA (46). Moreover, overexpression of any of the three classical LPA receptors or ATX in the mammary epithelium of mice is sufficient to promote late onset ER + mammary cancers (15), whereas overexpression of aromatase in the mammary epithelium results in hyperplasia, but no overt tumor formation (47). Despite these data, the role of mammary fat-derived LPA in TNBC biology has been far less explored. Here we model the mammary microenvironment to study the roles of the mammary fat-derived lipid-metabolites, LPC and LPA, in ER-negative breast cancer progression.

Novel ATX, LPAR and dual-activity inhibitors have been developed to decrease LPA signaling in cancer. These inhibitors are effective in attenuating primary tumor growth and inhibiting metastasis in xenografted breast cancer cells (33,34,37,48,49). Our data suggest that the anti-cancer effects of antagonizing LPA signaling are due in part to the blockade of LPA signals from the mammary fat pad. In this study, both LPA and LPC were identified as important metabolites secreted from mammary adipose tissue that provide proliferative and survival signals to ER- cancer cells. Furthermore, these data suggest that paracrine signals from cancerous epithelium increase expression of ATX in the mammary fat pad, both *in vitro* and *in vivo* (Supp. Fig. 2) and support the development of preventive therapies that target localized LPA signaling in the mammary microenvironment.

Our previous observations suggested that the physiological response to chronic social isolation in TAg female mice resulted in larger mammary tumors and increased expression of genes encoding enzymes mediating the production of specific lipids led us to perform an unbiased lipidomic analysis of the mammary fat from socially isolated versus group-housed animals. Of immediate interest was the significant elevation of LPC, the precursor to LPA that has been associated with increased breast tumorigenesis, in the mammary fat from socially-isolated mice. The goal of the current work was to examine the possible role of the signaling molecule LPA (the precursor of LPC) and ATX (the adipose tissue-secreted enzyme responsible for the generation of LPA from LPC) derived specifically from mammary gland fat, in promoting TNBC tumorigenesis. To further delineate these molecular relationships and model the mammary gland microenvironment, we employed an *in vitro* approach using MEC lines derived from various stages of TAg-induced mammary tumorigenesis, and mammary adipose tissue CM.

The TAg-initiated mammary cancer lines employed here are models for human TNBC progression. LPA addition to serum-free medium stimulated proliferation and survival in all three TAg MEC lines. However, CM experiments suggested that the importance of LPA as a proliferative/survival signal is context-dependent and may change with cancer progression. In the normal and CIS cells, LPAR1/3 antagonism by chemical inhibitors or RNA interference revealed that LPA signaling was a significant pro-proliferative component of the mammary adipose CM. The same set of experiments indicated that LPAR2 expression may be dispensable for the effects of the CM in all three TAg cell lines. However, the LPAR2 antagonist (H2L5186303) used in this study has only been validated in cell-based assays using LPA-induced Ca+ mobilization (50) and despite multiple attempts, we were unable to knockdown LPAR2 mRNA in the TAg cell lines using siRNA. Therefore, further work is required to firmly dismiss a role for LPAR2 in these cells.

Unlike normal and CIS cells, the M6 TAg invasive mammary cancer cells were not dependent on LPA for CM-induced proliferation. Blockade of LPAR-mediated signaling had no impact on the pro-proliferative effects of CM in these cells. In advanced cancers, acquired mutations may diminish the role of LPA in cell proliferation, while increasing its importance in migration, invasion, and metastasis (40). This hypothesis agrees with a previous study which found that decreasing LPA signaling to xenografts in a mouse model using a small molecule ATX antagonist significantly attenuated xenograft tumor growth in early-stage cancers, but the effect was lost in advanced cancers (38). Notably, ATX inhibition caused lung metastases to be decreased by 60%. Future investigation is needed to determine whether mammary fat-derived LPA directly influences tumor cell motility, invasion and/or metastasis.

A second property unique to the invasive TAg cancer cells was their ability to respond to the LPA precursor LPC, independently of its conversion to LPA. The mechanism through which LPC supports proliferation of the invasive TAg cell line is unclear. However, some aggressive fully transformed cancer cells acquire a phospholipid “scavenging” phenotype in which cell proliferation is supported by sequestered phospholipids that are then incorporated into cell membranes (51). The observation that only the invasive TAg cell line responded to LPC, independently of LPA generation/signaling, suggests that additional mutations during

breast cancer progression may contribute to acquiring LPC responsiveness. Indeed, the phospholipid scavenging phenotype has been associated with ras-transformed cells and ras pathway activation is characteristic of advanced TAg mammary tumors (51, 52). Acquired LPC responsiveness may therefore be an important therapeutic target in established TNBC.

It is known that cancer-associated adipocytes that are found adjacent to primary breast tumors, display an “activated” phenotype with elevated expression of specific proinflammatory cytokines and smaller, de-lipidated, cells (53). These activated adipocytes appear to modify cancer cell characteristics leading to a more aggressive tumor behavior (53). Our data suggest that increased ATX expression may be an important and targetable oncogenic mechanism used by cancer-associated adipocytes. For example, we observed a striking increase in ATX expression in the stromal-compartment of TAg vs. parental mouse mammary glands. Similar observations were made in two other studies, one in human breast cancer and the other in a mouse model (32, 38). In a panel of 87 invasive human breast carcinomas, Popnikolov et al. reported increased stromal ATX expression in 16.3% of samples, and high ATX expression was associated with strong desmoplastic stromal reactions (32). Benesch et al. reported that mammary fat pads engrafted with a tumor displayed about a 2-fold increase in ATX activity compared to the non-grafted contralateral fat pad (38). Interestingly, although the xenografted cancer cells studied expressed negligible ATX activity, inhibition of ATX attenuated primary xenograft growth and metastasis. The authors suggested that these effects were due to inhibition of ATX activity from the mammary fat pad. Consistent with the association between increased stromal ATX expression and cancerous mammary epithelium, our data implicate soluble factors secreted from TAg transformed epithelial cells in the increased ATX expression within the mammary fat pad. Future studies will examine inflammatory cytokines such as TNF-alpha as putative regulators of adipocyte ATX production (54, 55).

Cumulatively, our data suggest an important role for mammary adipocyte-derived LPA and ATX in ER-negative breast cancer progression, and support further investigation into the mechanisms underlying the link between mammary adipocytes and breast cancer progression in the TNBC subtype. These data also suggest there is bi-directional communication between mammary adipose tissue and breast cancer cells in upregulating the LPC/ATX/LPA axis, perhaps independently of obesity. Studies are ongoing to extend these findings by using primary human mammary adipose tissue CM and studying its effect on human TNBC cells lines. These data also support the continued development of strategies that target LPA production and signaling in the prevention and treatment of breast cancer.

Supplementary Material

Refer to Web version on PubMed Central for supplementary material.

Acknowledgments

We thank Joscelyn Hoffman and Hannah You for generously sharing their expertise with rodent husbandry. We thank Dr. Terri Li for providing immunohistochemical expertise. We thank Dr. Joe Sachleben for his guidance in the analysis of lipids. We also thank Dr. Gabrielle Baker for providing expert pathological analysis of our IHC samples.

Funding: This work was supported by NIH grants NIH R01-CA148814 to S.D. Conzen and M.K. McClintock, DOD Idea Award BC 061754 and U.S. Army W81XWH-07-1-0296 to M.K. McClintock, NIH 1 T32 DK087703 and a DOD pre-doctoral fellowship W81XWH-11-1-014901 to P. A. Volden, and by the University of Chicago Comprehensive Cancer Center (NIH P30 CA14599) supported cores: Pathology, Microscopic Imaging and NMR Cores. The lipidomics analyses were performed at the Kansas Lipidomics Research Center Analytical Laboratory. Instrument acquisition and lipidomics method development was supported by National Science Foundation (EPS 0236913, MCB 0920663, DBI 0521587, DBI1228622), Kansas Technology Enterprise Corporation, K-IDeA Networks of Biomedical Research Excellence (INBRE) of National Institute of Health (P20GM103418), and Kansas State University. Targeted LPA and LPC analyses were performed by the Wayne State Lipidomics Core Facility that is supported in part by the National Institutes of Health National Center for Research Resources (S10 RR027926).

References

1. Shekhar MPV, Pauley R, Heppner G. Host microenvironment in breast cancer development - Extracellular matrix-stromal cell contribution to neoplastic phenotype of epithelial cells in the breast. Breast Cancer Re. 2003; 5:130–35.
2. Roca-Rivada A, Alonso J, Al-Massadi O, Castelao C, Ramon Peinado J, Maria Seoane L, et al. Secretome analysis of rat adipose tissues shows location-specific roles for each depot type. Journal of Proteomics. 2011; 74:1068–79. [PubMed: 21439414]
3. O'Rourke RW, Metcalf MD, White AE, Madala A, Winters BR, Maizlin I, et al. Depot-specific differences in inflammatory mediators and a role for NK cells and IFN-gamma in inflammation in human adipose tissue. International Journal of Obesity. 2009; 33:978–90. [PubMed: 19564875]
4. Porter SA, Massaro JM, Hoffmann U, Vasan RS, O'Donnel CJ, Fox CS. Abdominal subcutaneous adipose tissue: a protective fat depot? Diabetes Care. 2009; 32:1068–75. [PubMed: 19244087]
5. Subbaramaiah K, Howe LR, Bhardwaj P, Du B, Gravaghi C, Yantiss RK, et al. Obesity Is associated with inflammation and elevated aromatase expression in the mouse mammary gland. Cancer Prev Res. 2011; 4:329–46.
6. Friedenreich CM. Review of anthropometric factors and breast cancer risk. European J Cancer Prev. 2001; 10:15–32. [PubMed: 11263588]
7. Ford NA, Devlin KL, Lashinger LM, Hursting SD. Deconvoluting the obesity and breast cancer link: secretome, soil and seed interactions. J of Mammary Gland Biology and Neoplasia. 2013; 18:267–75.
8. Humphreys RC, Lydon J, Omalley BW, Rosen JM. Mammary gland development is mediated by both stromal and epithelial progesterone receptors. Mol Endocrinology. 1997; 11:801–11.
9. Marzan CV, Kupumbati TS, Bertran SP, Samuels T, Leibovitch B, Mira-y-Lopez R, et al. Adipocyte derived paracrine mediators of mammary ductal morphogenesis controlled by retinoic acid receptors. Dev Biology. 2011; 349:125–36.
10. Landskroner-Eiger S, Park J, Israel D, Pollard JW, Scherer PE. Morphogenesis of the developing mammary gland: Stage-dependent impact of adipocytes. Dev Biology. 2010; 344:968–78.
11. Williams JB, Pang D, Delgado B, Kocherginsky M, Tretiakova M, Krausz T, et al. A model of gene-environment interaction reveals altered mammary gland gene expression and increased tumor growth following social isolation. Cancer Prev Res. 2009; 2:850–61.
12. Volden PA, Wonder EL, Skor MN, Carmean CM, Patel FN, Ye H, et al. Chronic Social Isolation Is Associated with Metabolic Gene Expression Changes Specific to Mammary Adipose Tissue. Cancer Prev Res. 2013; 6:634–45.
13. Houben AJS, Moolenaar WH. Autotaxin and LPA receptor signaling in cancer. Cancer and Metastasis Reviews. 2011; 30:557–65. [PubMed: 22002750]
14. Kitayama J, Shida D, Sako A, Ishikawa M, Hama K, Aoki J, et al. Over-expression of lysophosphatidic acid receptor-2 in human invasive ductal carcinoma. Breast Cancer Res. 2004; 6:R640–46. [PubMed: 15535846]
15. Liu SY, Umezu-Goto M, Murph M, Lu YL, Liu WB, Zhang F, et al. Expression of autotaxin and lysophosphatidic acid receptors Increases Mammary Tumorigenesis, invasion, and metastases. Cancer Cell. 2009; 15:539–50. [PubMed: 19477432]

16. Park S-J, Lee K-P, Kang S, Chung H-Y, Bae Y-S, Okajima F, et al. Lysophosphatidyl-ethanolamine utilizes LPA(1) and CD97 in MDA-MB-231 breast cancer cells. Cellular Signalling. 2013; 25:2147–54. [PubMed: 23838008]

17. Dusaulcy R, Gres S, Wanecq E, Rancoule C, Colom A, Guigne C, et al. The invalidation of the autotaxin adipocyte exacerbates obesity and nutrition reduces plasma lysophosphatidic acid. Diabetes & Metabolism. 2011; 37:A32–A32.

18. Ferry G, Tellier E, Try A, Gres S, Naime I, Simon MF, et al. Autotaxin is released from adipocytes, catalyzes lysophosphatidic acid synthesis, and activates preadipocyte proliferation - Up-regulated expression with adipocyte differentiation and obesity. J Biol Chem. 2003; 278:18162–69. [PubMed: 12642576]

19. Holzer RG, MacDougall C, Cortright G, Atwood K, Green JE, Jorcyk CL. Development and characterization of a progressive series of mammary adenocarcinoma cell lines derived from the C3(1)/SV40 Large T-antigen transgenic mouse model. Breast Cancer Res Treatment. 2003; 77:65–76.

20. Broussard JL, Ehrmann DA, Van Cauter E, Tasali E, Brady MJ. Impaired Insulin Signaling in Human Adipocytes After Experimental Sleep Restriction A Randomized, Crossover Study. Annals Int Med. 2012; 157:549–57.

21. Snijder B, Sacher R, Ramo P, Liberali P, Mench K, Wolfrum N, et al. Single-cell analysis of population context advances RNAi screening at multiple levels. Mol Systems Bio. 2012; 8:579.

22. Ramakers C, Ruijter JM, Deprez RHL, Moorman AFM. Assumption-free analysis of quantitative real-time polymerase chain reaction (PCR) data. Neuroscience Letters. 2003; 339:62–6. [PubMed: 12618301]

23. Schmittgen TD, Livak KJ. Analyzing real-time PCR data by the comparative C-T method. Nature Prot. 2008; 3:1101–08.

24. Guillou H, Zadravec D, Martin PGP, Jacobsson A. The key roles of elongases and desaturases in mammalian fatty acid metabolism: Insights from transgenic mice. Progress in Lipid Res. 2010; 49:186–99.

25. Matsuzaka T, Shimano H, Yahagi N, Kato T, Atsumi A, Yamamoto T, et al. Crucial role of a long-chain fatty acid elongase, Elovl6, in obesity-induced insulin resistance. Nature Med. 2007; 13:1193–202. [PubMed: 17906635]

26. Rahimi N, Saulnier R, Nakamura T, Park M, Elliott B. Role of hepatocyte growth-factor in breast-cancer - a novel mitogenic factor secreted by adipocytes. DNA and Cell Bio. 1994; 13:1189–97. [PubMed: 7811385]

27. Barone I, Catalano S, Gelsomino L, Marsico S, Giordano C, Panza S, et al. Leptin mediates tumor-stromal interactions that promote the invasive growth of breast cancer cells. Cancer Res. 2012; 72:1416–27. [PubMed: 22282662]

28. Alvarez-Llamas G, Szalowska E, de Vries MP, Weening D, Landman K, et al. Characterization of the human visceral adipose tissue secretome. Mol Cell Proteomics. 2007; 6:589–600. [PubMed: 17255083]

29. Boucharaba A, Serre CM, Gres S, Saulnier-Blache JS, Bordet JC, Guglielmi J, et al. Platelet-derived lysophosphatidic acid supports the progression of osteolytic bone metastases in breast cancer. J Clini Invest. 2004; 114:1714–25.

30. Du J, Sun CQ, Hu ZZ, Yang Y, Zhu YC, Zheng DT, Gu L, Lu XA. Lysophosphatidic acid induces MDA-MB-231 breast cancer cells migration through activation of PI3K/PAK1/ERK Signaling. Plos One. 2010; 5:e15940. [PubMed: 21209852]

31. David M, Ribeiro J, Descotes F, Serre CM, Barbier M, Murone M, et al. Targeting lysophosphatidic acid receptor type 1 with Debio 0719 inhibits spontaneous metastasis dissemination of breast cancer cells independently of cell proliferation and angiogenesis. International J Oncology. 2012; 40:1133–41.

32. Popnikolov NK, Dalwadi BH, Thomas JD, Johannes GJ, Imagawa WT. Association of autotaxin and lysophosphatidic acid receptor 3 with aggressiveness of human breast carcinoma. Tumor Biology. 2012; 33:2237–43. [PubMed: 22922883]

33. Parrill AL. Lysophosphatidic acid receptor agonists and antagonists (WO2010051053). Expert Opinion Therap Patents. 2011; 21:281–86.

34. Ohta H, Sato K, Murata N, Damirin A, Malchinkhuu E, Kon J, et al. Ki16425, a subtype-selective antagonist for EDG-Family lysophosphatidic acid receptors. Mol Pharm. 2003; 64:994–1005.
35. David M, Wannecq E, Descotes F, Jansen S, Deux B, Ribeiro J, et al. Cancer cell expression of autotaxin controls bone metastasis formation in mouse through lysophosphatidic acid-dependent activation of osteoclasts. Plos One. 2010; 5
36. Samadi N, Gaetano C, Goping IS, Brindley DN. Autotaxin protects MCF-7 breast cancer and MDA-MB-435 melanoma cells against Taxol-induced apoptosis. Oncogene. 2009; 28:1028–39. [PubMed: 19079345]
37. Gierse J, Thorarensen A, Beltey K, Bradshaw-Pierce E, Cortes-Burgos L, Hall T, et al. A novel autotaxin inhibitor reduces lysophosphatidic acid levels in plasma and the site of inflammation. J Pharm Exp Ther. 2010; 334:310–17.
38. Benesch MG, Tang X, Maeda T, Ohhata A, Zhao YY, Kok BP, et al. Inhibition of autotaxin delays breast tumor growth and lung metastasis in mice. FASEB J. 2014; 28:2655–66. [PubMed: 24599971]
39. Tan J, Buache E, Chenard MP, Dali-Youcef N, Rio MC. Adipocyte is a non-trivial, dynamic partner of breast cancer cells. International J Dev Bio. 2011; 55:851–59.
40. Yom CK, Lee KM, Han W, Kim SW, Kim HS, Moon BI, et al. Leptin as a potential target for estrogen receptor-positive breast cancer. J Breast Cancer. 2013; 16:138–45. [PubMed: 23843844]
41. Brown KA. Impact of obesity on mammary gland inflammation and local estrogen production. J Mamm Gland Bio Neoplasia. 2014; 19:183–89.
42. Lonning PE, Haynes BP, Dowsett M. Relationship of body mass index with aromatisation and plasma and tissue oestrogen levels in postmenopausal breast cancer patients treated with aromatase inhibitors. European J Cancer. 2014; 50:1055–64. [PubMed: 24507547]
43. Patani N, Martin LA. Understanding response and resistance to oestrogen deprivation in ER-positive breast cancer. Mol Cell Endo. 2014; 382:683–94.
44. Rancoule C, Dusaulcy R, Treguer K, Gres S, Guigne C, Quilliot D, Valet P, Saulnier-Blache JS. Depot-specific regulation of autotaxin with obesity in human adipose tissue. J Physiol Bioch. 2012; 68:635–44.
45. Barber MN, Risis S, Yang C, Meikl PJ, Staples M, Febbraio MA, et al. Plasma Lysophosphatidylcholine Levels Are Reduced in Obesity and Type 2 Diabetes. Plos One. 2012:7.
46. Dusaulcy R, Rancoule C, Gres S, Wanecq E, Colom A, Guigne C, van Meeteren LA, Moolenaar WH, Valet P, Saulnier-Blache JS. Adipose-specific disruption of autotaxin enhances nutritional fattening and reduces plasma lysophosphatidic acid. Journal of Lipid Research. 2011; 52:1247–55. [PubMed: 21421848]
47. Kirma N, Gill K, Mandava U, Tekmal RR. Overexpression of aromatase leads to hyperplasia and changes in the expression of genes involved in apoptosis, cell cycle, growth, and tumor suppressor functions in the mammary glands of transgenic mice. Cancer Res. 2001; 61:1910–18. [PubMed: 11280746]
48. Swaney JS, Chapman C, Correa LD, Stebbins KJ, Bundey RA, Prodanovich PC, et al. A novel, orally active LPA(1) receptor antagonist inhibits lung fibrosis in the mouse bleomycin model. British J Pharm. 2010; 160:1699–13.
49. Zhang H, Xu X, Gajewiak J, Tsukahara R, Fujiwara Y, Liu J, Fells JI, Perygin D, Parrill AL, Tigyi G, Prestwich GD. Dual activity lysophosphatidic acid receptor pan-antagonist/autotaxin inhibitor reduces breast cancer cell migration in vitro and causes tumor regression in vivo. Cancer Res. 2009; 69:5441–49. [PubMed: 19509223]
50. Fells JI, Tsukahara R, Fujiwara Y, Liu J, Perygin DH, Osborne DA, et al. Identification of non-lipid LPA(3) antagonists by virtual screening. Bioorg & Med Chem. 2008; 16:6207–17. [PubMed: 18467108]
51. Kamphorst JJ, Cross JR, Fan J, de Stanchina E, Mathew R, White EP, et al. Hypoxic and Ras-transformed cells support growth by scavenging unsaturated fatty acids from lysophospholipids. Proc Natl Acad Sci USA. 2013; 110:8882–87. [PubMed: 23671091]
52. Green JE, Shibata MA, Yoshidome K, Liu ML, Jorcyk C, Anver MR, et al. The C3(1)/SV40 T-antigen transgenic mouse model of mammary cancer: ductal epithelial cell targeting with multistage progression to carcinoma. Oncogene. 2000; 19:1020–27. [PubMed: 10713685]

53. Dirat B, Bochet L, Dabek M, Daviaud D, Dauvillier S, Majed B, et al. Cancer-associated adipocytes exhibit an activated phenotype and contribute to breast cancer invasion. Cancer Res. 2011; 71:2455–65. [PubMed: 21459803]

54. Boucher J, Quilliot D, Praderes JP, Simon MF, Gres S, Guigne C, et al. Potential involvement of adipocyte insulin resistance in obesity-associated up-regulation of adipocyte lysophospholipase D/autotaxin expression. Diabetologia. 2005; 48:569–77. [PubMed: 15700135]

55. Benesch MGK, Zhao YY, Curtis JM, McMullen TPW, Brindle DN. Regulation of autotaxin expression and secretion by lysophosphatidate and sphingosine 1-phosphate. J Lipid Res. 2015; 56:1134–44. [PubMed: 25896349]

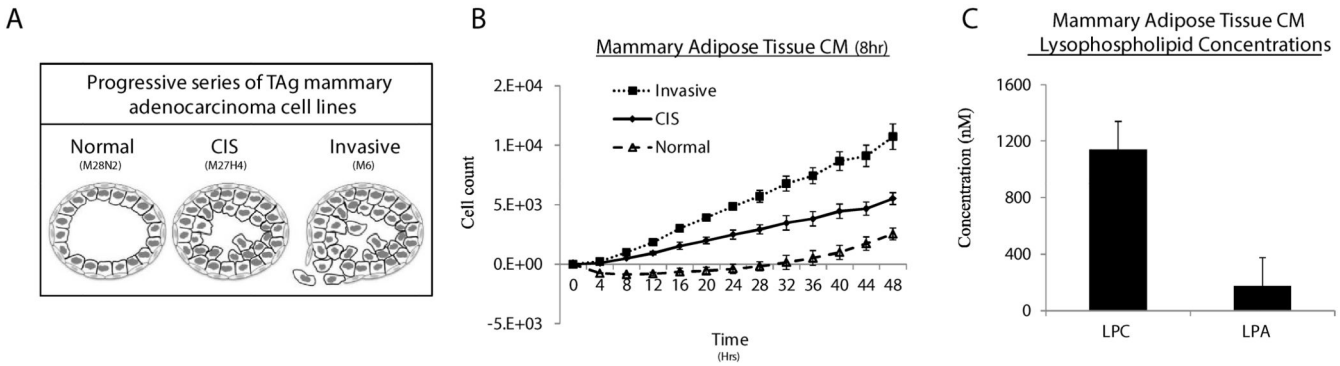

Figure 1.

Mammary adipose tissue conditioned medium (CM) contains LPC and LPA and supports the proliferation of TAg MECs. A, Diagram illustrating th TAg MEC lines and the representative cancer stage from which each cell line was obtained. B, Mammary adipose tissue was cultured in serum-free medium for 8hr to make conditioned (CM), which was then applied to TAg cell lines. Cell proliferation was measured using the Incucyte™ live content imaging system. Cell numbers were calculated from confluence values (see methods) and the data were plotted with the cell count at time=0 subtracted from all subsequent cell counts. Data represent means from two independent experiments for each cell line. C, Quantitative LC-MS analysis of LPC and LPA concentrations in 8hr mammary CM (n=5).

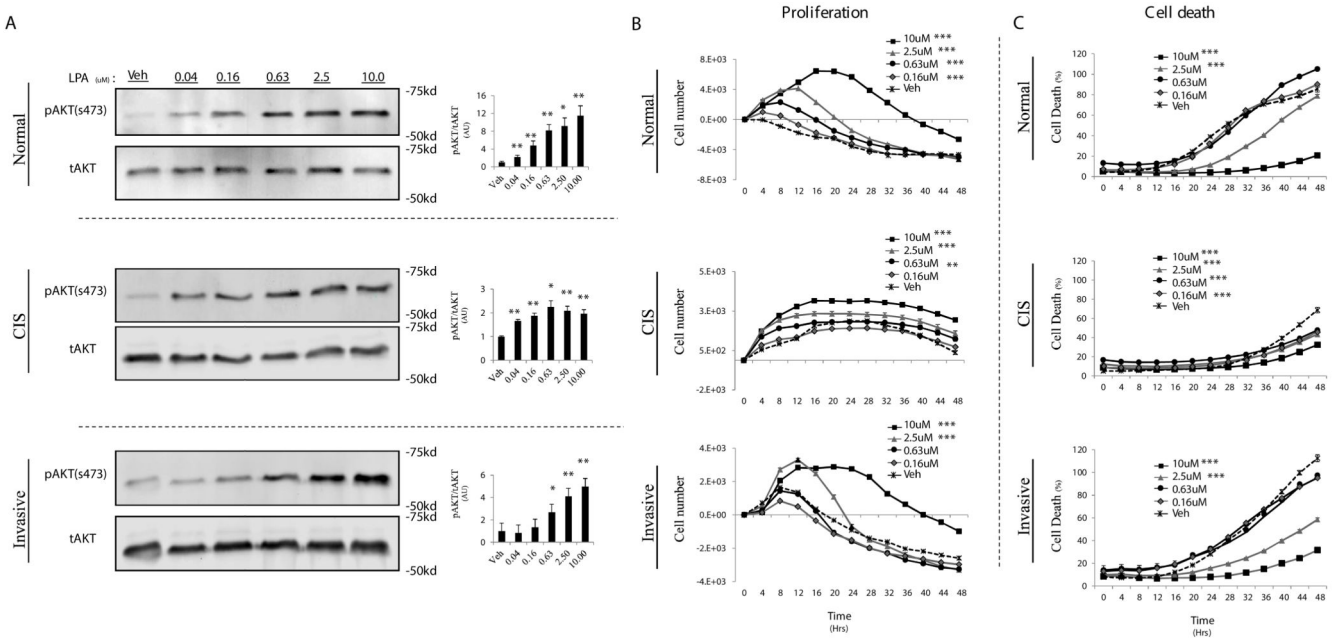

Figure 2.

LPA initiates a proliferative and survival signal for TAg MECs. A, TAg cell lines were serum starved for 8hr, followed by a 10 minute treatment with the indicated concentration of LPA. AKT phosphorylation at serine 473 (pAKT) levels was quantified by densitometry analysis of Western blots and normalized to total AKT levels (right, pAKT/AKT) (A). TAg cell lines were cultured without serum +/− the indicated concentration of LPA and then cell proliferation (B) and cell death (C) were measured using the Incucyte™ live content imaging system. LPA was only added at the initiation of the experiment. Cell numbers were calculated from confluence values (described in methods). Change in cell number was calculated by subtracting the initial cell count at treatment time=0 from all subsequent cell counts. Error bars indicate standard error of the mean. Statistics were determined from 3 independent experiments. In all panels; *, p≤ 0.05; **, p≤0.01; *** p≤0.001.

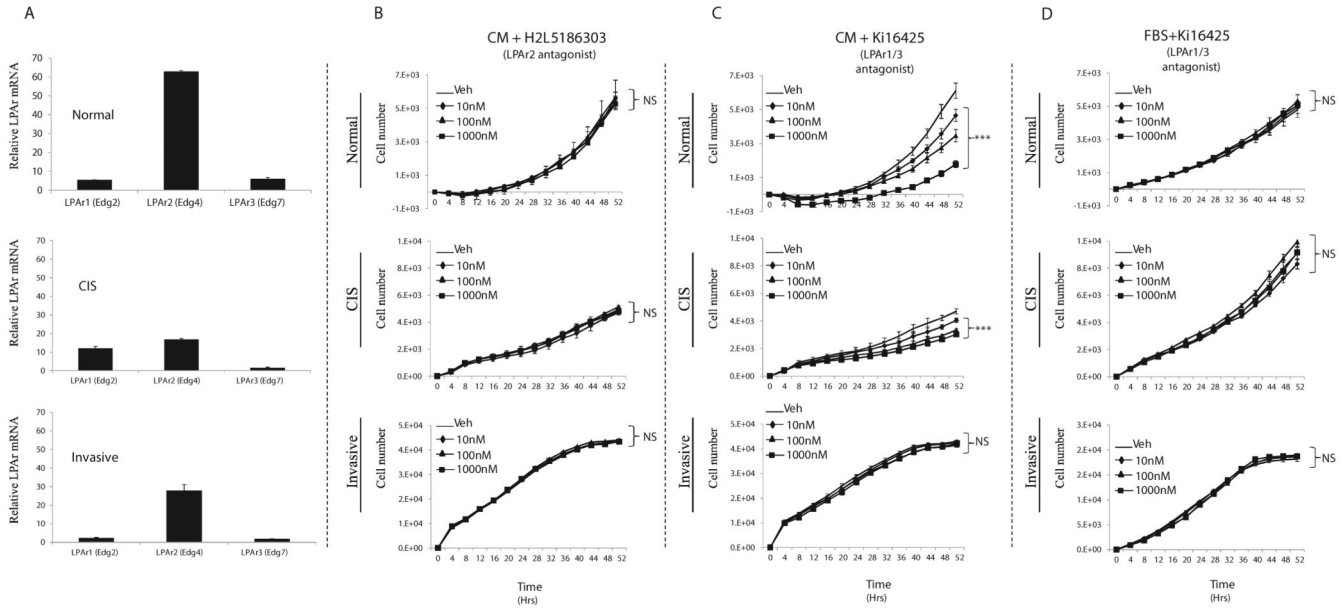

Figure 3.

LPAR 1/3 antagonism attenuates CM-induced TAg cell proliferation. A, Relative LPAR expression in TAg cell lines determined by q-RT-PCR. B, Proliferation of TAg cell lines cultured in mammary CM with the indicated dose of the LPAR2 antagonist, H2L5186303. C, Proliferation of TAg cell lines cultured in mammary CM with the indicated dose of the LPAR1/3 antagonist, Ki16425. D, Proliferation of TAg cell lines cultured 10% FBS medium with the indicated dose of the LPAR1/3 antagonist, Ki16425. . Statistics were determined from 3 independent experiments. Error bars indicate standard error of the mean. Panels B-D; NS, Not Significant; ***, p≤0.001 compared to vehicle (control).

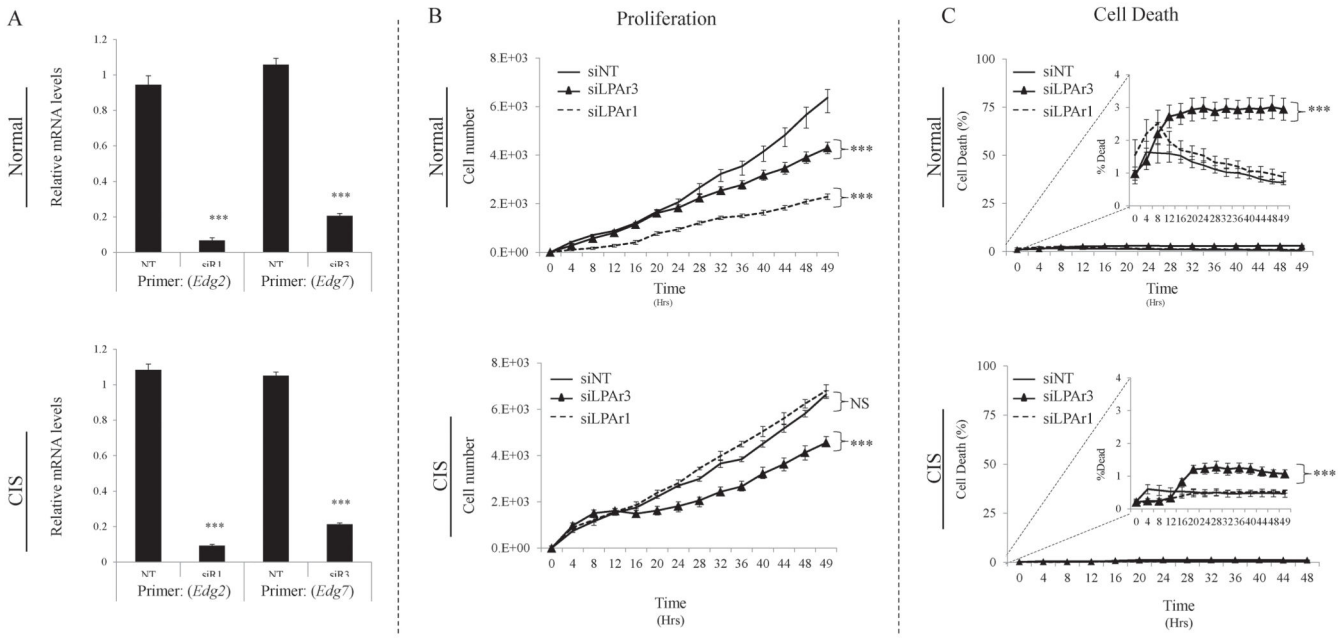

Figure 4.

MEC LPAR 1 and 3 signaling contributes to mammary adipose tissue CM pro-proliferative and pro-survival effects. A, Relative mRNA expression of LPAR1 and LPAR3 transcripts (*Edg2* and *Edg7*, respectively) following 48hr treatment with siRNAs targeting LPAR1 (siR1), LPAR3 (siR3), or non-targeting siRNA (NT). Following 48hr treatment with siRNAs targeting LPAR1, LPAR3, or non-targeting siRNAs, TAg MECs were washed and medium changed to mammary CM. Proliferation (B) and cell death (C) were measured in the Incucyte™ live content imaging system. . Statistics were determined from 3 independent experiments. Error bars indicate standard error of the mean. In all panels; ***, p≤0.001 compared to non-targeting siRNA (control).

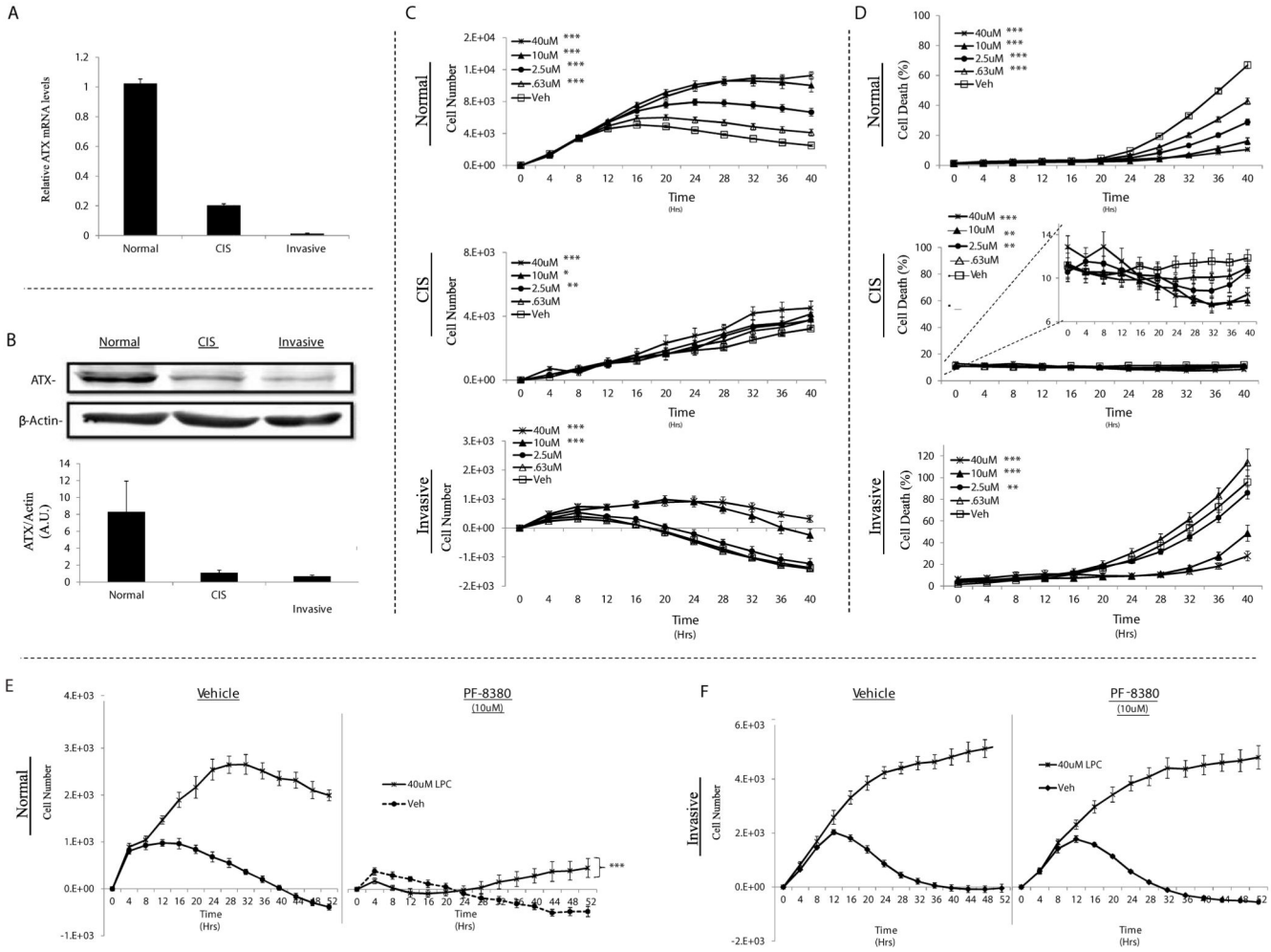

Figure 5.

LPC supports the proliferation and survival of TAg MECs and requires LPAR signaling in normal but not invasive TAg MECs. Relative expression of *ATX* (*Enpp2*) mRNA transcripts (A) and protein (B) in TAg cell lines. TAg cell lines were cultured without serum +/− the indicated concentration of LPC and then cell proliferation (C) and cell death (D) were monitored using the Incucyte™ live content imaging system. Normal (E) and invasive (F) TAg cell lines that were cultured without serum and in the presence or absence of 40uM LPC were treated with 10uM PF-8380 (ATX antagonist) or vehicle. The cells were then placed in the Incucyte™ live content imaging system to measure proliferation for 52 hours. Statistics were determined from 3 independent experiments. Error bars indicate standard error of the mean. Panels C - E; *, p≤0.05; **, p≤0.01; *** p≤0.001 compared to vehicle (control).

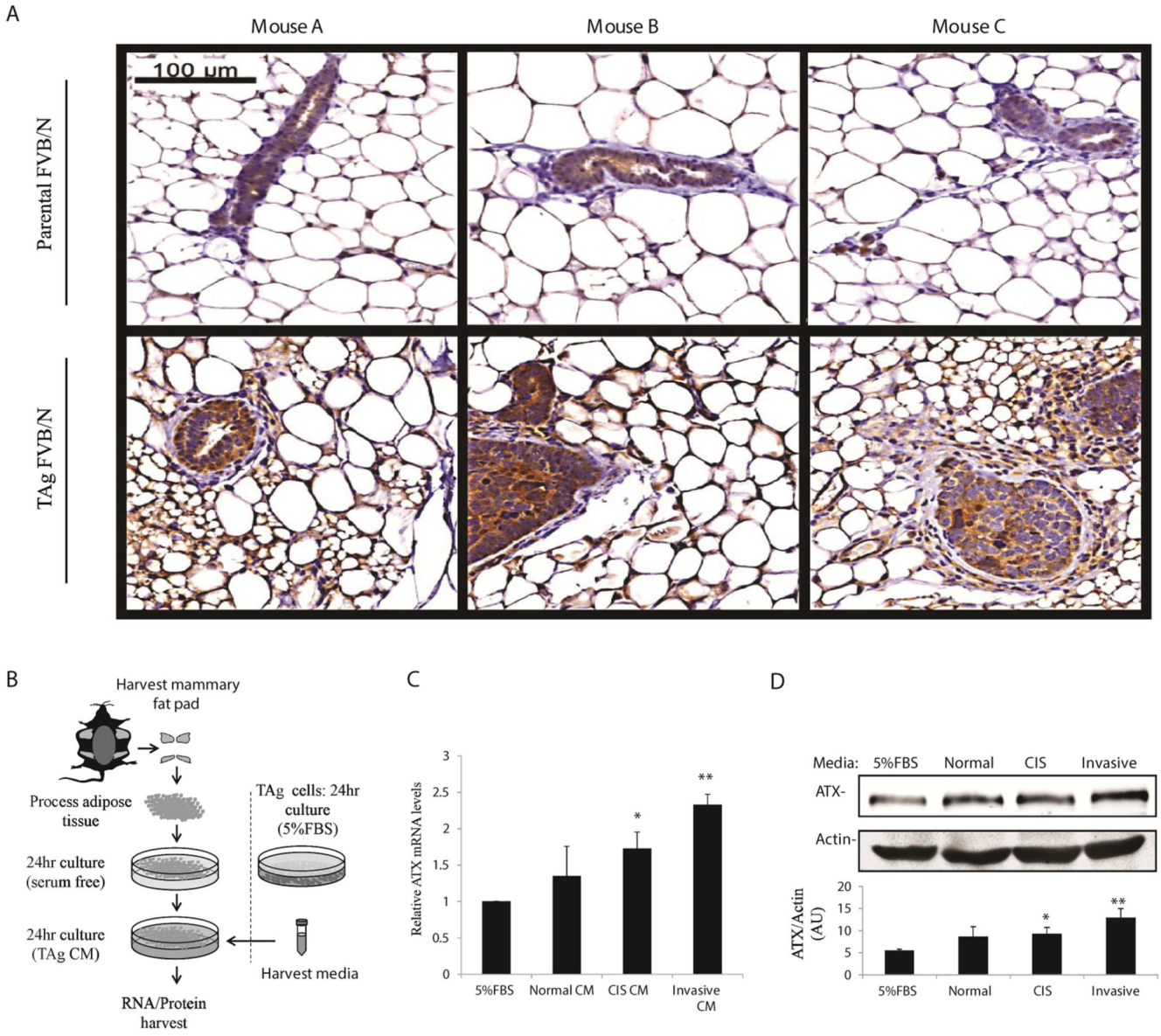

Figure 6.

TAg MEC-secreted factors induce ATX expression in mammary adipose tissue. A, Anti-ATX immunohistochemistry was performed on formalin-fixed paraffin-embedded mammary fat pads harvested from 15 week old TAg mice and the non-transgenic (parental) FVB/N line. Representative images from 3 different TAg and parental mice are shown. B, CM from each of the TNBC TAg cell lines was applied separately to mammary adipose tissue for 24 hours and then mammary fat RNA and protein were harvested. C, *ATX (Enpp2)* mRNA expression in mammary adipose tissue following 24hr exposure to TAg cell CM. D, ATX protein expression from mammary adipose tissue following 24hr exposure to TAg MEC line CM. Statistics were determined from 3 (ATX mRNA expression) and 4 (ATX protein

expression) independent experiments. Error bars indicate standard error of the mean. Panels C and D; *, $p \leq 0.05$; **, $p \leq 0.01$ compared to FBS (control).